Journal of the European Ceramic Society 23 (2003) 499–503

www.elsevier.com/locate/jeurceramsoc

Liquid-phase redistribution during sintering of 8 mol% yttria-stabilized zirconia

Young-Soo Jung, Jong-Heun Lee*, Je Hun Lee, Doh-Yeon Kim

School of Materials Science and Engineering, and Center for Microstructure Science of Materials, Seoul National University, Seoul 151-744, South Korea

Received 8 February 2002; accepted 12 April 2002

Abstract

The distribution of the intergranular liquid phase during the sintering of 8 mol% Y_2O_3-stabilized ZrO_2 containing 0.5 mol% of SiO_2 and Al_2O_3 was investigated using spatially resolved impedance spectroscopy. The variation in the grain-boundary resistivity as a function of the distance from the specimen surface indicated that the liquid phase coagulates at the specimen center in the initial stages of sintering, and spreads outward upon further sintering. The liquid redistribution was also examined by transmission electron microscopy. © 2002 Elsevier Science Ltd. All rights reserved.

Keywords: Grain boundaries; Impedance spectroscopy; Ionic conductivity; ZrO_2

1. Introduction

During the sintering of a ceramic material, the presence of a small amount of liquid phase, either intentionally added or formed by impurities, is known to enhance the sintering rate by providing a path for rapid material transfer.[1] Microstructural evolution during liquid-phase sintering has been thoroughly investigated and it has been shown that at the very early stage of sintering, liquid agglomerates at the center of a specimen to reduce the liquid–vapor interfacial energy.[2–4] Furthermore, the agglomerated liquid flows outward upon further sintering and consequently the whole specimen recovers a uniform microstructure.[2]

In this respect, the liquid phase is dynamic during sintering.[5] This makes it imperative to know its distribution change in order to understand the sintering process. For typical liquid-phase sintering with a relatively abundant liquid, such a liquid rearrangement process could be observed using scanning electron microscopy (SEM).[2–4,6,7] However, when the liquid content is very small, SEM becomes inappropriate because the liquid usually presents as an intergranular film of a few nm in thickness.

The sintering of yttria stabilized zirconia (YSZ) is usually carried out with a small amount of SiO_2, whether it is included as an inevitable background impurity[8] or is added on purpose,[9] which becomes liquid at the sintering temperature. Note also that the ionic conductivity YSZ is very sensitive to the intergranular liquid and the impedance values depend strongly on its configuration.[10,11] In this study, the rearrangement process of the small amount of liquid phase during sintering was investigated. For this purpose, the variation in the local impedance of the 8 mol% yttria-stabilized zirconia (8YSZ) specimens sintered at various conditions was determined.

2. Experimental procedure

High purity 8YSZ powder (TZ-8Y, Tosoh Co. Ltd., Tokyo, Japan) was used as a raw material. The impurity contents with regard to Al_2O_3, SiO_2, Fe_2O_3, and Na_2O were, according to the manufacturer's specification, <0.1, 0.02, 0.01, and 0.12 wt.%, respectively. With the addition of 0.5 mol% of Al_2O_3 powder (AKP3000, Sumitomo Chemical Co., Tokyo, Japan) and 0.5 mol% of SiO_2 sol (MA-ST-M, Nissan Chemical Co., Tokyo,

* Corresponding author. Tel.: +82-2-880-6981; fax: +82-2-884-1413.

E-mail address: jongheun@gong.snu.ac.kr (J.-H. Lee).

PII: S0955-2219(02)00151-6

Japan), the mixture was ball-milled for 6 h in ethanol using partially stabilized zirconia balls. After drying, 5.2 g of the powder was uniaxially pressed into a cylindrical rod shaped specimen then isostatically pressed at 200 MPa. The compacts were sintered at 1450–1550 °C for 0–4 h in air. Sintering for 0 h means that the specimen was cooled immediately after the sintering temperature was reached. The heating and cooling rates were fixed to 200 °C/h. A pure 8YSZ specimen was also fabricated as a comparison. The sample specifications, sintering conditions, average grain sizes, and densities are shown in Table 1.

Fig. 1 shows a schematic illustration of the electrode configuration on the sintered specimen. A slab, $10.6\times10.5\times0.55$ mm^3, was obtained by cutting along the diameter. The 6 electrodes were made from the surface to the center with a 0.5 mm spacing by screen printing a Pt paste (TR 7905, Tanaka Co., Tokyo, Japan). The size of each rectangular electrode was 2×0.5 mm^2. After drying, the specimen was heat-treated at 1100 °C for 1 h. Spatially resolved impedance data was measured at 400 °C in air by an AC two-probe technique using a SI 1260 impedance/gain-phase analyzer (Model No. SI 1260, Solartron, Inc., Farnborough, UK). The experimental setup for the impedance measurement is reported elsewhere.[12] The microstructure of the intergranular liquid was analyzed by TEM (JEM 3000F, 300kV, Jeol Ltd., Japan). The average grain size of the specimen was determined by multiplying the average intercept length by 1.755.[13]

3. Results and discussion

Fig. 2 shows the complex impedance spectra of the 1450–0 specimen (sintered at 1450 °C for 0 h) as a function of the distance from the surface, d. Three contributions from the low frequency regime are those from electrode polarization, the grain boundary, and the grain interior, respectively. The grain-boundary resistivity (ρ_{gb}) varied to a large extent with d while the grain-interior resistivity (ρ_{gi}) was a constant as 6 kΩ·cm. Because the electrode area and conduction length normalized impedance, the deconvoluted ρ_{gb} value does not represent the specific grain-boundary resistivity (ρ_{gb}^{sp}). The estimation of the ρ_{gb}^{sp} value was difficult due to the variation in the intergranular film thickness or the space charge layer. Therefore, the resistance per unit grain-

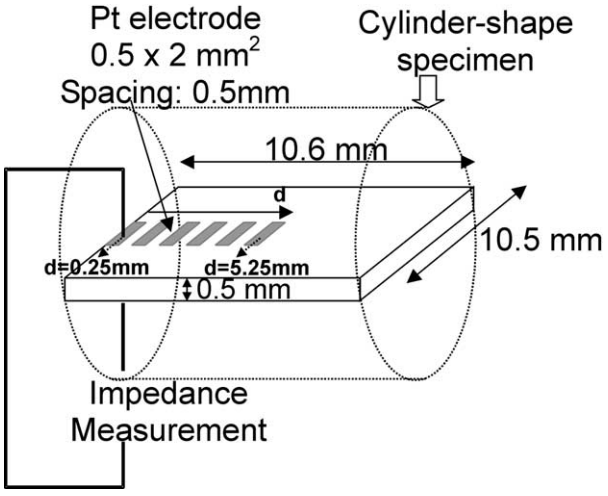

Fig. 1. Schematic diagram of the electrode configuration on the specimen for measuring the spatially resolved impedance (d: distance from the surface).

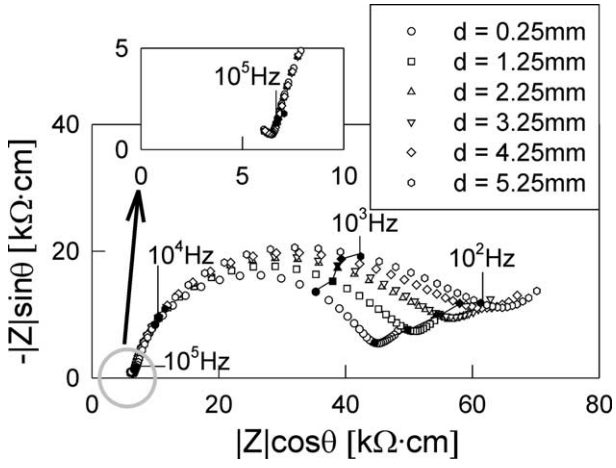

Fig. 2. Spatially resolved impedance spectra of the specimen sintered at 1450 °C for 0 h (1450–0 specimen) as a function of the distance from the surface, d (measured at 400 °C in air).

Table 1
Specifications, starting materials, sintering conditions, densities and the average grain sizes of the specimens

Specimen	Composition		Sintering condition	Density[a] (g/cm^3)	d_g [b] (μm)
1450–0	8YSZ + 0.5 mol%	Al_2O_3 + 0.5 mol% SiO_2	1450 °C for 0 h	5.83	4.5
1550–0	8YSZ + 0.5 mol%	Al_2O_3 + 0.5 mol% SiO_2	1550 °C for 0 h	5.98	5.9
1550–4	8YSZ + 0.5 mol%	Al_2O_3 + 0.5 mol% SiO_2	1550 °C for 4 h	6.02	29.4
P1450–0	8YSZ		1450 °C for 0 h	5.74	2.8

[a] Apparent density, as measured by Archemedes' method.
[b] Average grain size, as determined by linear intercept method.

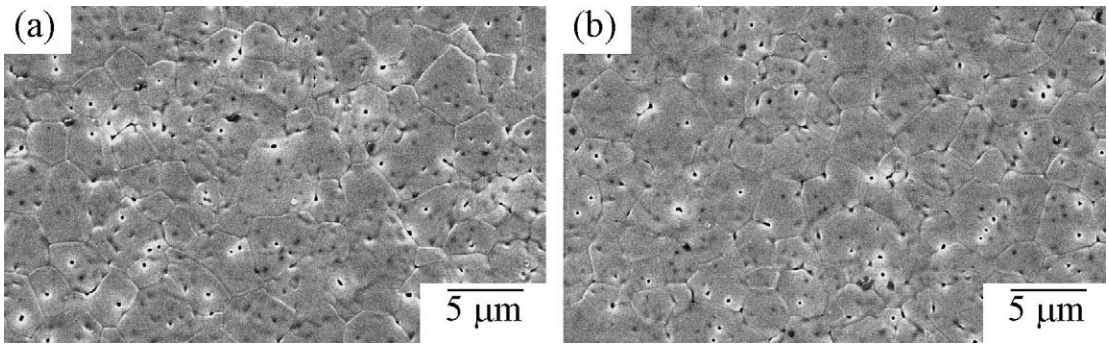

Fig. 3. SEM microstructures of the (a) surface and (b) center of the 1450–0 specimen.

boundary area (R_{gbs}) was calculated in this study by the following equation[14]

$$R_{gbs} = \rho_{gb}/D \quad (1)$$

Here, D is the grain-boundary density (number of grain boundaries per unit length), which is the reciprocal of the average grain size.

Fig. 3(a) and (b) shows SEM microstructures of the surface and the center of the 1450–0 specimen, respectively. No significant difference in the grain size was found, which suggests that the variation in the ρ_{gb} values in Fig. 2 does not emanate from the difference in the grain-boundary density. Further detailed information regarding the intergranular film such as its presence or absence, its thickness and configuration was difficult to obtain by SEM.

All the other specimens in this study showed no variation in grain size between the surface and the center. The R_{gbs} values were calculated from the local ρ_{gb} values and are plotted in Fig. 4. The R_{gbs} variation with d changed significantly with the sintering conditions. For the 1450–0 specimen [Fig. 4(a)], the R_{gbs} value increased with d and was saturated at $d > 2$ mm. As shown in Fig. 4(b), the R_{gbs} profile for the specimen sintered at 1550 °C for 0 h showed no variation with d. This tendency was kept after sintering for 4 h at 1550 °C but the overall R_{gbs} values increased [Fig. 4(c)]. These results were confirmed by repetitive measurements.

Fig. 4(d) shows the R_{gbs} profile for the pure 8YSZ specimen that was sintered at 1450 °C for 0 h (P1450–0 specimen). The R_{gbs} values were uniform and approximately 4.5 $\Omega \cdot cm^2$. For the same specimen, the R_{gbs} profile was also uniform after sintering at 1550 °C. Note that the R_{gbs} values of the P1450–0 sample are approximately 1% of those of the 1550–4 sample. This points to the intergranular liquid as the main cause of grain-boundary resistance. Therefore, the change in the R_{gbs} profile with the sintering conditions should be found in the framework of the intergranular-liquid distribution.

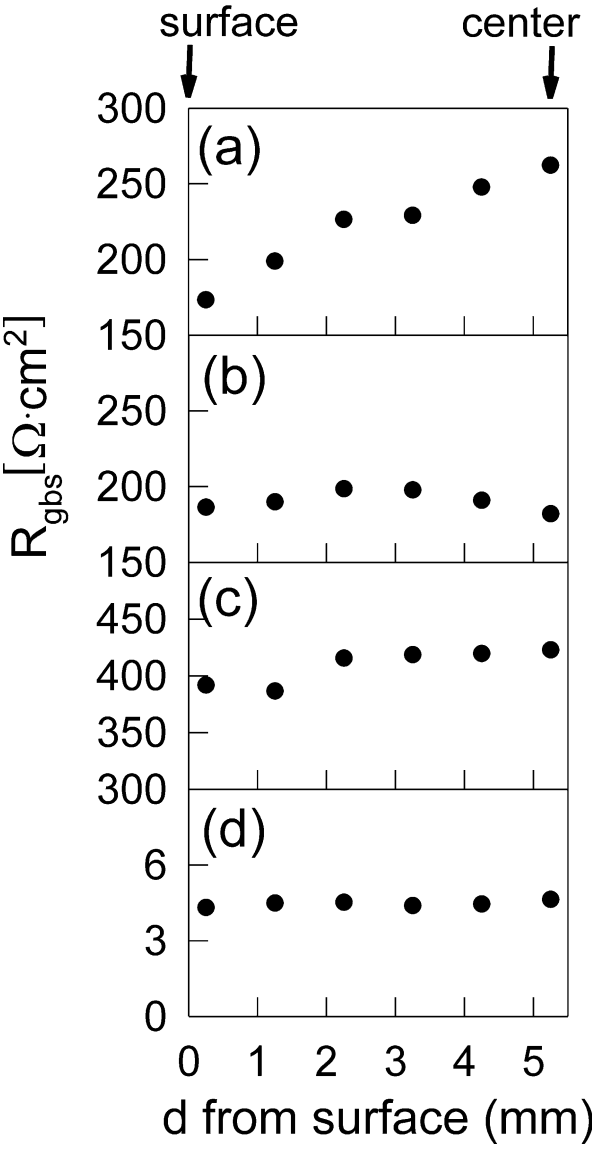

Fig. 4. The variation in the resistance per unit grain-boundary area (R_{gbs}) as a function of the distance from the surface, d, of the (a) 1450–0, (b) 1550–0, (c) 1550–4 and (d) P1450–0 specimens (measured at 400 °C in air).

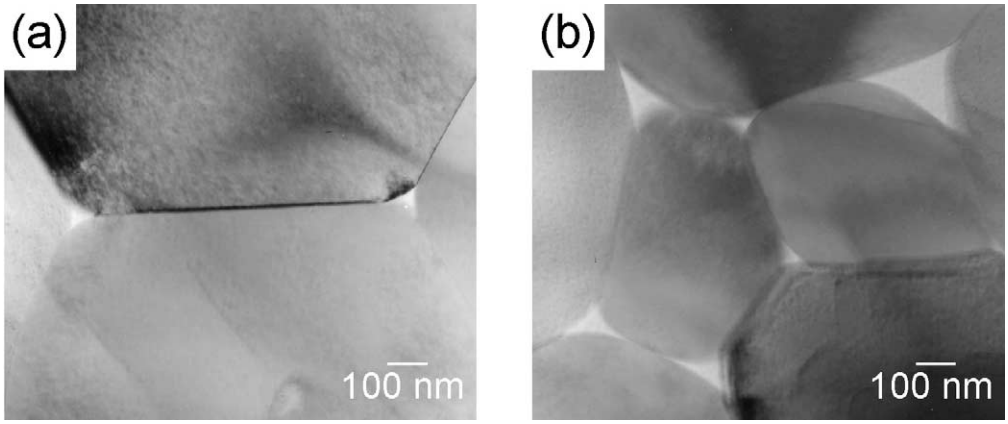

Fig. 5. Typical configuration of the intergranular liquid in the (a) surface and (b) center region of the 1450–0 specimen.

The higher R_{gbs} values at the center of the 1450–0 specimen, which compare to those of the surface, are expected to be a consequence of liquid coagulation at the center. On the other hand, the uniform R_{gbs} values in the 1550–0 and 1550–4 specimens suggest the liquid phase is again uniformly distributed. Liquid coagulation at the initial stages of liquid-phase sintering and its subsequent homogenization has been reported in several systems.[2–4] For example, when mixtures of W and 1 wt.% of Ni powders were sintered, liquid Ni was observed to agglomerate initially at the specimen center to decrease the total liquid–vapor interface area then spread outward with further densification.[2] As shown in the Table 1, the 1450–0 specimen showed the lowest density compared to the 1550–0 and 1550–4 specimens. The 1450–0 specimen is believed to be in the initial stages of sintering.

Fig. 5(a) and (b) shows the intergranular liquid configuration observed by TEM at the surface and in the center of the 1450–0 specimen, respectively. For each region, more than 30 liquid pockets and grain boundaries were examined. At the surface of the specimen, approximately all the liquid was confined to the triple junctions. In contrast, the size of liquid pocket is larger in the specimen center than at the specimen surface and the penetration of liquid along the grain boundaries is frequently noted. This observation supports the premise that the liquid content at the center of the 1450–0 specimen is higher than at the surface. Therefore, the higher R_{gbs} values at the center of the 1450–0 sample are a natural consequence of such liquid coagulation. The results show that the liquid phase is dynamic and rearranges during sintering even when its amount is quite small.

4. Conclusions

The rearrangement process of the intergranular liquid during sintering of an 8 mol% Y_2O_3-stabilized zirconia specimen was estimated by measuring the local impedance. The analysis showed that the intergranular liquid coagulated in the center of the specimen in the initial stages of sintering then spread outward as densification proceeded. The local impedance measurements were sensitive enough to predict the change in the spatial distribution of the small amount of liquid in the stabilized zirconia.

Acknowledgements

This work was supported by the Korea Research Foundation Grant (KRF 2001–003-E00369).

References

1. German, R. M., *Liquid Phase Sintering*. Plenum Press, New York, 1985 pp. 1–11.
2. Kwon, O.-J. and Yoon, D. N., The liquid phase sintering of W–Ni. In *Sintering and Related Phenomena*, ed. G. C. Kuczynski. Plenum Publishing Company, 1980, pp. 203–218.
3. Yoo, Y.-S., Kim, J.-J. and Kim, D.-Y., Effect of heating rate on the microstructural evolution during sintering of $BaTiO_3$ ceramics. *J. Am. Ceram. Soc.*, 1987, **70**, C322–C324.
4. Kim, Y. S., Park, J. K. and Yoon, D. N., Liquid flow into the interior of W–Ni–Fe compacts during liquid phase sintering. *Int. J. Powder Metall.*, 1985, **21**, 30–37.
5. Shaw, T. M., Liquid redistribution during liquid-phase sintering. *J. Am. Ceram. Soc.*, 1986, **69**, 27–34.
6. Park, H.-H., Cho, S.-J. and Yoon, D.-N., Pore filling process in liquid phase sintering. *Metall. Trans. A*, 1984, **15A**, 1075–1080.
7. Kwon, O.-J. and Yoon, D. N., Closure of isolated pores in liquid phase sintering of W–Ni. *Int. J. Powder Metall.*, 1981, **17**, 127–133.
8. Lee, J.-H., Mori, T., Li, J.-G., Ikegami, T., Komatsu, M. and Haneda, H., Improvement of grain-boundary conductivity of 8 mol% yttria-stabilized zirconia by precursor scavenging of siliceous phase. *J. Electrochem. Soc.*, 2000, **147**, 2822–2829.
9. De Souza, D. P. E. and De Souza, M. F., Liquid phase sintering of Re_2O_3: YSZ ceramics, Part I. Grain growth and expelling of the grain boundary glass phase. *J. Mater. Sci.*, 1999, **34**, 4023–4030.

10. Gödickemier, M., Michel, B., Orliukas, A., Bohac, P., Sasaki, K., Gauckler, L., Henrich, H., Schwander, P., Kostorz, G., Hofmann, H. and Frei, O., Effect of intergranular glass films on the electrical conductivity of 3Y-TZP. *J. Mater. Res.*, 1994, **9**, 1228–1240.
11. Lee, J.-H., Mori, T., Li, J.-G., Ikegami, T. and Takenouchi, S., Impedance spectroscopic estimation of inter-granular phase distribution in 15 mol% calcia-stabilized zirconia/alumina composites. *J. Eur. Ceram. Soc.*, 2001, **21**, 13–17.
12. Lee, J.-H., Lee, J. H. and Kim, D.-Y., The inhomogeneity of grain-boundary resistivity in calcia-stabilized zirconia. *J. Am. Ceram. Soc.*, 2002, **85**, 1622–1624.
13. Han, J.-H. and Kim, D.-Y., Analysis of the proportionality constant correlating the mean intercept length to the average grain size. *Acta Metall. Mater.*, 1995, **43**, 3183–3188.
14. Miyayama, M., Yanagida, H. and Asada, A., Effect of Al_2O_3 addition on resistivity and microstructure of yttria-stabilized zirconia. *Am. Ceram. Soc. Bull.*, 1986, **65**, 660–664.